Gravity Recovery and Climate Experiment (GRACE) Derived Water Equivalent Changes of the Arctic Watersheds

C51C-0493

Reginald R. Muskett & Vladimir E. Romanovsky, The Geophysical Institute, University of Alaska Fairbanks, USA

C51C-0493

ABSTRACT

The Arctic permafrost regions compose the largest component of the cryosphere. Observations from the Gravity Recovery and Climate Experiment (GRACE) mission offer to provide a greater understanding of changes in water mass within these regions. We investigate GRACE monthly time series, snow water equivalent from the Special Scanning Microwave Imager (SSM/I), and discharge from the Lena, Yenisei, Ob', Mackenzie and Yukon River watersheds. GRACE water equivalent mass change respond to mass loading by snow accumulation in winter and mass unloading by runoff in spring. Comparison of secular trends from GRACE to runoff indicates groundwater storage is increasing in the Lena and Yenisei watersheds, decreasing in the Mackenzie and Yukon watersheds, and is steady in the Ob' watershed. We also note that groundwater storage is increasing in the Alaska Arctic coastal plain. We hypothesize that the groundwater storage changes are linked to the development of closed talik (unfrozen material acting as aquifers) in the continuous permafrost zone and decrease of permafrost lateral extent and new open talik formation in the discontinuous permafrost zone of the watersheds. The increase in talik may be linked to increase in surface and sub-surface water associated with thaw bogs, ponds, lakes and river-beds in the continuous permafrost zone and decrease in surface and sub-surface water associated with draining of thaw bogs, ponds and lakes in the discontinuous permafrost zone.

Introduction

Permafrost is the largest component of the cryosphere (Zhang et al., 1999). Degradation of ice-rich permafrost can lead to significant surface subsidence affecting changes in ecosystem, landscape, and where human habitats are established, significant infrastructure damage (Romanovsky and Osterkamp, 1997; Osterkamp and Romanovsky, 1997). The processes of freezing and thawing, growth and degradation of permafrost, affects the land surface energy and moisture fluxes (balances) which in turn impact biogeochemical cycles, climate and hydrologic systems (Romanovsky and Osterkamp, 1997; Sergueev et al., 2003; Romanovsky et al., 2007).

In the Arctic terrestrial regions hydrologic processes are controlled by the presence or absence of permafrost and the thickness of the active layer (Romanovky and Osterkamp, 1997; Osterkamp and Romanovsky, 1997; White et al., 2007; Zhang et al., 2008). Talik is unfrozen earth material formed by hydrothermal and thermal processes near and beneath the ground surface within permafrost (Woo, 1993). Wildfires in boreal forest and tundra can disturb the underlying permafrost and active layer leading to talik formation (Yoshikawa, et al., 2003). Closed talik can be laterally extensive within permafrost. It can occur beneath lakes and rivers crossing the continuous and discontinuous permafrost zones. Open talik within permafrost connects the ground surface to the unfrozen material beneath permafrost allowing for recruitment of surface water into groundwater storage and loss of groundwater storage into surface water. In wintertime, baseflow of rivers in permafrost watersheds is maintained by water leaving groundwater storage (Sergueev et al., 2003; Chapin et al., 2006; Buldovich et al., 2008). Liquid water residing within cold and warm permafrost affects the ground thermal state (Romanovsky and Osterkamp, 2000). The effect is largest near the ground surface and active layer after freeze-up, with stronger thermal gradients at the ground surface and increased heat flux.

Diverse observations across the high-latitude northern hemisphere indicate permafrost temperatures at about 2 meters depth have increased over the twentieth century (Romanovsky et al., 2007). These are correlated well to surface air temperature changes on decadal time scales. Permafrost temperatures in eastern Siberia and northern Alaska have shown the largest magnitude of increases of a few degrees centigrade. Increased surface air temperatures from climate warming over the same period often cannot fully account forincreased permafrost temperatures, suggesting that variability in snow cover may be a contributing factor (Osterkamp, 2007). Satellite data suggest that the total area of thermokarst lakes increased up to 12% in the northern continuous permafrost zone in western Siberia through processes of degradation of permafrost, and the number of all lakes increased by 4% over the last 30 years (Smith et al., 2005). However, in the southern discontinuous, sporadic and isolated permafrost zones showed in lake area losses up to 13% and the number of lakes decreased up to 9%

Global satellite observations from the Gravity Recovery and Climate Experiment (GRACE) have shown to be great promise in detecting secular trends and spatial-temporal variations in land and ocean hydrologic mass balance (equivalent water thickness change) since the operational period beginning in August 2002 and ongoing (Tapley et al., 2004; Wahr et al., 2004, 2006; Chambers, 2006). We investigate the GRACE observations for addressing permafrost, talik and active layer change in the Lena and Ob-Irtysh River watershed regions in Eurasia and the Mackenzie and Yukon River watershed regions in North America (Fig. 1). In addition, we will show analysis of water equivalent mass changes on the Arctic coastal plain in Alaska.

Figure 1. Arctic permafrost watersheds and distribution of permafrost zones.

Data Sets

GRACE Water Equivalent Mass Changes

The co-orbiting satellites of the Gravity Recovery and Climate Experiment (GRACE) do not measure the variations of the inter-satellite range (range rate and range acceleration), coupled with accurate GPS location relative to the International Terrestrial Reference Frame 2005, to estimate values of the time change in spherical harmonic geopotential coeficients, ΔC and ΔS, to degree and order 120 (the Level-3 grids are complete to degree and order 40) (Chambers, 2006). These are then used in the expansion below to estimate movement of water mass:

$$\Delta h(\phi,\lambda,t) = \frac{a_e \rho_e}{3\rho_w} \sum_{l=0}^{40} \sum_{m=0}^{l} \frac{(2l+1)}{(1+k_l)} W_l P_{lm} \sin\phi \, [\Delta C_{lm}(t)\cos m\lambda + \Delta S_{lm}(t)\sin m\lambda]$$

$$W_l = \exp\left[\frac{(lr/a_e)^2}{4\ln(2)}\right]$$

P_{lm} : Normalized Legendre polynomials

ΔC_{lm}, ΔS_{lm} : Normalized time-varying Stokes spherical harmonic Geopotential coeficients

a_e -- Earth mean radius; ρ_e -- Earth mean density; ρ_w -- Density of water; r -- Spatial radius; t -- Time; ϕ, λ -- Latitude and longitude; k_l -- Love numbers

The GRACE Release 4 Level-3 300 km smoothing kernal land and ocean monthly grids, from August 2002 through March 2008, were combined to give global coverage, then adjusted by a Glacial Isostatic Adjustment grid (Paulson et al., 2007). Figure 2. Shows the GRACE water equivalent thickness changes on the terrestrial portion of the northern hemisphere for September 2006, and May 2007. These were chosen to illustrate the spatial non-uniform distribution of the seasonal amplitude range of terrestrial sourced regions. The GRACE water equivalent mass changes on the northern hemisphere show that the permafrost watersheds have a seasonal cycle minimum in September and maximum in May in anti-phase with the mass changes of the Arctic Ocean.

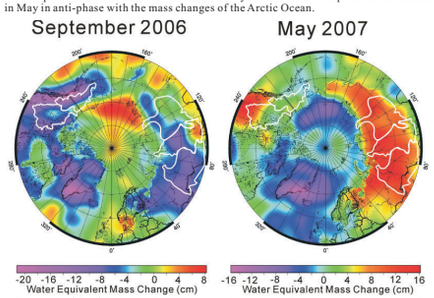

Figure 2. GRACE-derived water equivalent mass changes on the northern hemisphere. The Arctic permafrost watersheds are shown by area-extents; Yukon and Mackenzie (N. America) and Lena, Yenisei and Ob' (Eurasia). The months of September and May are the seasonal minimum and maximum, respectively, of water mass change on the Arctic permafrost watersheds. Interestingly, these months are in anti-phase to the seasonal cycle of water equivalent mass changes of the Arctic Ocean.

High-Resolution Hybrid Geoid Models

Since the early 1990s the NOAA National Geodetic Survey have been working on developmentsof high-spatial resolution and high-accuracy geoid models as part of the U.S. national mapping and geodetic control network modernization programs (Smith and Milbert, 1999; Smith and Roman, 2001). The efforts centered on producing hybrid geoid models using gravimetric geoid observations (within the U.S. and territorial coastal waters), the U.S. High-Accuracy Reference Network with Global Position System station coordinate determinations and long-wavelength undulations from the Earth Gravity Model 1996 (EGM96) (Lemoine et al., 1998) 360 degree and order 15 arc-minute by 15 arc-minute model and realization with respect to the International Terrestrial Reference Frame (ITRF) in the non-tide geodetic reference convention. The first hybrid model 2 arc-minute by 2 arc-minute grid was GEOID-1996 (GEOID96) with a 5.5 cm vertical accuracy. It was followed in 1999 by the 1 arc-minute by 1 arc-minute model GEOID99 with a 4.6 cm vertical accuracy. Hybrid models GEOID03 and GEOID06 followed. The latest efforts have produced GEOID09 which incorporates EGM-2008, a 2159 degree and order 1 arc-minute by 1 arc-minute model (http://www.ngs.gov/GEOID/USGG2009/tech.html). Early testing was indicating a 1.5 cm vertical accuracy. Furthermore, we use vertical rate data from continuous operating GPS stations in Alaska and Yukon relative to the International Terrestrial Reference Frame 2005 to estimate an adjustment for elastic effects (which are removed from geoid differences in the analysis of water equilent changes).

Snow Water Equivalent Changes

Global snow water equivalent estimates on a monthly time basis derive from the NOAA Defense Meteorological Satellite Program by the Special Sensor Microwave/Imagers (SSM/I), are proveded by the National Snow and Ice Data Center (http://nsidc.org/data/docs/dac/nsidc_0271_ease_grid_swe_climatology.gd.html). SSMI and its predecessor instrument, has been retrieving passive microwave data since 1978. Snow Water Equivalent (SWE) estimates in units of millimeters were derived using the horizontally polarized difference algorithm for the 19 and 37 GHz channels from daily orbit swath acquisitions (Chang et al., 1987). Daily retrievals are averaged to compose monthly estimates. Missing retrievals due to swath coverage gaps are interpolated from neighboring swaths. Sensor resolution is about 69 by 43 square kilometers. The monthly data are gridded in the equal-area Ease-grid projection system at about 25-by-25 kilometer grid intervals.

Watershed Runoff

Eurasian and North American based measurements (at gauging stations) of surface water discharge (runoff) in the watersheds were provided by ArcticRIMS (daily/monthly provisional data from 2000 through 2009), R-Arctic-NET (archive monthly data from 1930 through 2000), Arctic Freshwater Systems and the U.S. Geological Survey. Monthly discharge from stations at Kusur (Lena), Igarka (Yenisei), Salekhard (Ob'), Arctic Red River (Mackenzie), Pilot Station (Yukon), Umiat (Colville), and stations near Dead Horse and Prudhoe Bay (Kuparuk nad Sagavanirktok) wereused. The archival periods of the discharged records of each watershed stations used varies in total number of years; Kusur covered a period from 1935 through 2000, Igarka covered a period from 1936 through 1999, Salekhard covered a period from 1930 through 1999, and Arctic Red River covered a period from 1972 through 2000. The archival records were compared to the provisional records to help identify discharge anomalies. We then derived annual time series of runoff by summing the monthly runoff from August through July periods. August through July was chosen as this period coincided with the GRACE time series instead of the typical water-year calendar convention. Runoff volume, in cubic meters is converted to water equivalent thickness by dividing by the watershed area in square meters.

Results

Figure 3 shows comparisons of area-averaged time series of sample mean and standard deviation, and least-squares regression trends of the Lena, Yenisei, Ob', Yukon and Mackenzie permafrost watershed regions. Take notice of the trends (+ or -) and percentage of permafrost per watershed.

Eurasian Watersheds

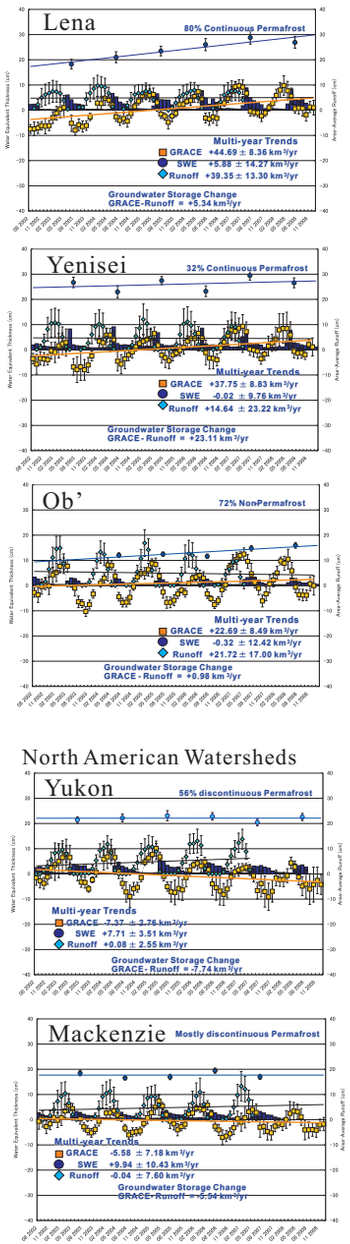

North American Watersheds

Figure 3. Time series of GRACE (water equivalent mass change),SWE and Runoff. Estimates of groundwater storage change are given.

GRACE, SSM/I and Runoff Trends and Variations

GRACE-derived water equivalent mass changes show response to winter water mass loading, derived through SSM/I, and spring water mass unloading derived by watershed runoff in Figure 3 (Muskett and Romanovsky, 2009). Water mass loading preceeds the peak in GRACE by about one to two months. Water mass unloading (runoff) in June produces the sharp drop after seasonal peak in the GRACE time series, lending to asymmetric sinusoidal character.

Groundwater storage change is estimated by subtracting runoff trend from the GRACE trend in each watershed;

$$\Delta\text{Groundwater Storage} \cong \text{GRACE - Runoff.}$$

This indicates increasing groundwater storage in the Eurasian watersheds and decreasing groundwater storage in the North American watersheds (Muskett and Romanovsky, 2009).

High-Resolution Geoid Difference Changes in the Alaska Arctic coastal plain and the Yukon River Watershed in Alaska, U.S.A, and Yukon Territory, Canada

To obtain high spatial resolution (1 arc-minute) water equivalent mass changes, we difference the NOAA National Geodetic Survey geoid models GEOID99 (1999 epoch) and GEOID09 (2009 epoch), with adjustment for post-glacial and neotectonic effects by using vertical coordinate GPS-ITRF2005 data at network stations in Alaska and Yukon. The resultant geoid difference map shows the net water equivalent changes from 1999 through 2009 (Fig. 4 on the left). We compare this to a GRACE-difference map (Fig. 4 on the right). The area of the Yukon River watershed is given. The high-resolution geoid-difference area-average mass balance compares closely to the GRACE area-average least-squares trend. Tables 1 and 2 show trends on the Alaska Arctic coastal plain (continuous permafrost) and the Yukon River watershed (mostly discontinuous permafrost).

Table 1. Multi-Year Trends of GRACE (water equivalent mass), SSM/I (snow water equivalent) and Runoff from August 2002 through December 2008, Arctic coastal plain and foothills, and Yukon River watershed.

A. Total Volume Change Rates

Region	GRACE	SSM/I	Runoff
Arctic Coastal Plain	+0.06 ± 0.14 km^3/a	+0.82 ± 0.36 km^3/a	-1.14 ± 0.31 km^3/a
Arctic Foothills	-0.99 ± 0.25 km^3/a	+0.56 ± 0.42 km^3/a	-1.14 ± 0.31 km^3/a
Yukon Watershed	-7.37 ± 2.76 km^3/a	+7.17 ± 3.51 km^3/a	+0.08 ± 2.55 km^3/a

B. Area-Average Thickness Change Rates

Region	GRACE	SSM/I	Runoff
Arctic Coastal Plain	+0.05 ± 0.13 cm/a	+0.78 ± 0.35 cm/a	-1.10 ± 0.31 cm/a
Arctic Foothills	-0.99 ± 0.25 cm/a	+0.56 ± 0.42 cm/a	-1.10 ± 0.31 cm/a
Yukon Watershed	-0.78 ± 0.29 cm/a	+0.63 ± 0.38 cm/a	+0.01 ± 0.38 cm/a

In A. and B. runoff on the Alaskan Arctic coastal plain and foothills is integrated using the discharges from the Colville River (Umiat Station), Kuparuk River (Deadhorse), and Sagavanirktok River (Pump Station #3).

Table 2. Groundwater storage Changes from GRACE and Geoid Difference Mass Balance

A. Total Volume Change Rates

Region	GRACE Groundwater Storage Trend	Geoid Difference
Arctic Coastal Plain	+1.15 ± 0.65 km^3/a	+2.95 ± 1.97 km^3/a
Arctic Foothills	+0.11 ± 0.68 km^3/a	-0.14 ± 1.37 km^3/a
Yukon Watershed	-7.44 ± 3.76 km^3/a	-7.06 ± 1.04 km^3/a

B. Area-Average Thickness Change Rates

Region	GRACE Groundwater Storage Trend	Geoid Difference
Arctic Coastal Plain	+1.10 ± 0.62 cm/a	+2.83 ± 1.89 cm/a
Arctic Foothills	+0.11 ± 0.48 cm/a	-0.13 ± 0.98 cm/a
Yukon Watershed	-0.79 ± 0.40 cm/a	-0.78 ± 0.11 cm/a

Groundwater Storage Trend on the Yukon River Watershed

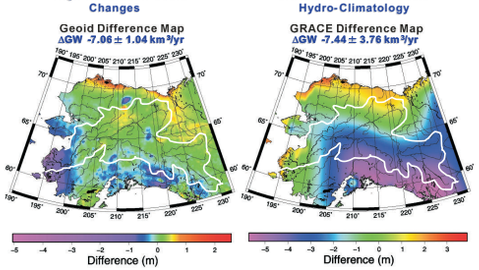

1999 to 2009 | 12 2004 to 7 2008

Figure 4. A comparison of spatial variation of groundwater storage changes derived through high resolution (1 arc minute) geoid model difference and the continental scale (1 degree arc) GRACE trend. The high resolution difference includes an adjustment of isostatic solid body effects derived from GPS-IRTF2005 vertical velocities at stations in Alaska and Yukon.

Conclusions

In this investigation we have made comparisons of the GRACE water equivalent mass changes (mass balance) with the SSM/I SWE changes, on a nominal monthly basis from August 2002 through December 2008. The discordance of the Least-squares time regression trends of GRACE and SSM/I SWE, lack of correlation of variation, and differences of timing in their seasonal cyclesindicates that the source of the GRACE water mass change on the Arctic permafrost watershed regions is not due to surface snow water change. The seasonal loading-unloading of vegetation water content is small, hence the source of the GRACE water mass changes must lie in the subsurface.

GRACE-derived groundwater storage shows water equivalent mass gains in the Eurasian watersheds and water equivalent mass losses in the North American watersheds (Figs. 3 and 4, Tables 1 and 2). We interpret these changes are being facilitated by development and growth of new and existing taliks in the continuous permafrost zone and accompanied by degradation of permafrost in the discontinuous permafrost zone. The development and growth of new and existing taliks is occurring beneath thaw ponds and lakes and riverbeds. In the continuous permafrost zone beneath thaw ponds and lakes, the development and growth of new closed taliks is increasing groundwater storage capacity. Increasing active layer thickness from thaw settlement (beneath water bodies) is hypothesized. In the discontinuous permafrost zone the development and growth of new and existing open taliks, leading to loss of groundwater storage (thaw lake drainage) is hypothesized.

Acknowledgements

This work was funded through supporting grants from NASA (NNOG6M48G), the National Science Foundation (NSF) ARC0632400 and ARC0856864 projects, Alaska EPSCoR NSF award #EPS-0701898 and the State of Alaska. The managers and participants in the ArcticRIMS, Arctic Freshwater systems and U.S. Geological Survey are thanked for providing hydrologic datasets. The Alaska Region Supercomputing Center is thanked for providing computing facilities support. The Japan Aerospace Exploration Agency is thanked for Linux cluster computing support. GRACE data were processed by D.P. Chambers, supported by the NASA Earth Science REASoN GRACE Project (http://grace.jpl.nasa.gov). G. Grosse is thanked for discussion of new thaw pond, lake and pingo formation on the Arctic coastal plain of Alaska. R.R. Muskett performed this research at the International Arctic Research Center.

References

Buldovich, S., N. Romanovskii, G. Tipenko, D. Sergeev, and V. Romanovsky (2008), Permafrost dynamics within an upper Lena River tributary: Modeled impact of infiltration on the temperature field under a plateau, in Proceedings of the Ninth International Conference on Permafrost June 29-July 3 Fairbanks, Alaska, 1 211-214, University of Alaska Fairbanks Institute of Northern Engineering, AK, U.S.A.

Chambers, D. (2006), Observing seasonal steric sea level variations with GRACE and satellite altimetry, J. Geophys. Res., 111, C03010, doi:10.1029/2005JC002914.

Chang, A.T.C., J.L. Foster, and D.K. Hall (1987), Nimbus-7 SMMR derived global snow cover parameters Annals of Glaciol., 9, 39-44.

Chapin, III, F.S, D. McGuire, R.W. Ruess, M.W. Walker, R.D. Boone, M.E. Edwards and twenty-two others (2006), Summary and Synthesis: Past and Future Changes in the Alaskan Boreal Forest, in F.S. Chapin III et al. [Eds.], Alaska's Changing Boreal Forest, 332-338, Oxford Univ. Press Inc., Oxford, U.K.

Lemoine, F.G., S.C. Kenyon, J.K. Factor, R.G. Trimmer, N.K. Palvis, and 10 others (1998), The Development of the Joint NASA GSFC and the National Imagery and Mapping Agency (NIMA) Geopotential Model EGM96, NASA Goddard Space Flight Center, NASA/TP1998206861, 575 pp., Maryland, U.S.A.

Muskett, R.R. and V.E. Romanovsky (2009), Groudwater storage changes in arctic permafrost watersheds from GRACE and in-situ measurements. *Environ. Res. Lett.*, 4, doi:10.1088/1748-9326/4/4/045009.

Osterkamp, T.E. (2007), Charasteristics of the recent warming of permafrost in Alaska, *J. Geophys. Res.*, 112, F02S02, doi: 10.1029/2006JF000578.

Paulson, A., S. Zhong, and J. Wahr (2007), Inference of mantle viscosity from GRACE and relative sea level data, *Geophys. J. Int.*, 171: 497-508, doi: 10.1111/j.1365.246X.2007.03556.x.

Romanovsky, V.E., and T.E. Osterkamp (1997), Thawing of the active layer on the coastal plain of Alaskan Arctic, Perm. & Peri. Process., 8 (1), 1-22.

Romanovsky, V.E., and T.E. Osterkamp (2000), Effects of unfrozen water on heat and mass transport processes in the active layer and permafrost, Perm. & Peri. Process. 11 (3), 219-239.

Romanovsky, V.E., T.S. Sazonova, V.T. Balohaev, N.I. Shender, and D.O. Sergueev (2007), Past and recent changes in air and permafrost temperatures in eastern Siberia, *Global & Planet. Change*, 56, 399-413, doi: 10.1016/j.gloplacha.2006.07.023.

Sergueev, D.O., G.S. Tipenko, V.E. Romanovsky, and N.N. Romanovskii (2003), Evolution of mountain permafrost as a result of long-term climate change (in Russian), Earth Cryosphere, 7 (2), 15-22.

Smith, D.A., and D.G. Milbert (1999), The GEOID96 high-resolution geoid height model for the United States, J. Geod., 73, 219-236.

Smith, D.A., and D.R. Roman 2001 GEOID99 and G99SSS: 1-arc-minute geoid models for the United States, J. Geod., 75, 469-490.

Smith, L.C., Y. Sheng, G.M. MacDonald, and L.D. Hinzman (2005), Disappearing Arctic lakes, Science, 308, 5727, 1429, doi:10.1126/science.1108142.

Tapley, B.D., S. Bettadpur, J.C. Ries, P.F. Thompson, and M.M. Watkins (2004), GRACE measurements of mass variability in the Earth system, *Science*, 305 (5683), doi:10.1126/Science.1099192.

Wahr, J., S. Swenson, V. Zlomicki, and I. Velicogna (2004), Time-variable gravity from GRACE: First results, *Geophys. Res. Lett.*, 31, L11501, doi: 10.1029/2004GL019779.

Wahr, J., S. Swenson, and I. Velicogna (2006), Accuracy of GRACE mass estimates, *Geophys. Res. Lett.*, 33, L06401, doi: 10.1029/2005GL025305.

White, D., L. Hinzman, L. Alessa, J. Cassano, M. Chambers, K. Falkner, J. Francis, W. J. Gutowski Jr, M. Holland, R. Max Holmes, H. Huntington, D. Kane,m A. Kliskey, C. Lee, J. McClelland, B. Peterson, T. Scott Rupp, F. Straneo, M. Steele, R. Woodgate, D. Yang, K. Yoshikawa, and T. Zhang (2007), The arctic freshwater system: Changes and impacts, *J. Geophys. Res.*, 112, G04S54, doi: 10.1029/2006JG000353.

Woo, M.-K. (1993), Northern Hydrology in Canada's Cold Environments, H.M. French and O. Slaymarker [Eds.], 117-142, McGill-Queen's Univ. Press, Montreal and Kingston, CA.

Zhang, T., R.G. Berry, R.G. Knowles, J.A. Heginbottom, and J. Brown (1999), Statistics and characteristics of permafrost and ground-ice distribution in the Northern Hemisphere, Polar Geograph., 23, 132-154.